

Interaction of K^+ Mesons with Emulsion Nuclei; K^+ Energy Range 140–375 Mev*

B. SECHI ZORN AND G. T. ZORN
 Brookhaven National Laboratory, Upton, New York
 (Received June 6, 1960)

Experimental data are presented on the interaction in nuclear emulsions of K^+ mesons in the energy range 140–375 Mev.

From an optical-model calculation based on a Wood-Saxon potential ($r_0=1.15A^{1/3}$ f, $d=0.57$ f), the real K nuclear potential V was found to be positive (or repulsive), varying from 18.5 ± 3.3 Mev at the lowest energy to 13.5 ± 5.0 Mev at the highest energy. The value of the imaginary nuclear potential W changed with increasing energy from -12.9 ± 1.4 Mev to -17.6 ± 2.5 Mev.

The K -nucleon cross section was derived from the imaginary nuclear potential and, under the assumption of the independent-particle model of the nucleus, the total K -neutron noncharge-exchange cross section σ_{Kn^+} and the charge-exchange cross section

σ_{Kn^0} were determined. It was found that σ_{Kn^+} decreases with increasing energy from 12.1 ± 1.6 mb to 8.1 ± 1.5 mb, whereas σ_{Kn^0} increases from 4.6 ± 1.2 mb to 10.3 ± 2.4 mb.

A phase-shift analysis using the total cross sections σ_{Kp^+} (the K -proton cross section), σ_{Kn^0} , $\bar{\sigma}_{nb}$ (the average K -nucleon cross section), and V gave evidence for P -wave contribution in isotopic spin state $T=0$ and permitted an investigation of the angular distribution for K^+ -neutron scattering.

Charged π -meson production by K^+ mesons has been observed, and the K -nucleon cross section at ~ 280 -Mev K^+ energy was estimated to be $\sim 1/7$ mb.

I. INTRODUCTION

THE object of this investigation has been to study the nuclear interaction of high-energy K^+ mesons. The K energy interval chosen was 140 Mev to 375 Mev and the detector was nuclear emulsions.¹ In this experiment, three stacks were exposed, one at the Cosmotron and two at the Bevatron, in separated K^+ beams. A length of 286 meters of K track was followed and the events observed were classified, using standard emulsion techniques, as elastic scattering, inelastic scattering with and without K charge exchange, decays in flight, and K -hydrogen scatterings. The experimental results were found to be in general agreement with those reported by other investigators.²⁻⁴

The analysis of the results was directed at understanding the K -nucleus and K -nucleon interactions and was, therefore, principally concerned with the elastic and inelastic K -nucleus scatterings. This study was carried out in three energy intervals into which the experimental results were divided.

The basis of this analysis was the optical model of the nucleus.⁵ In this model the nucleus is considered as a scattering center characterized by a Coulomb potential, a real nuclear potential V , and an imaginary nuclear

potential W . From a comparison of experimental results on elastic and inelastic scattering with those calculated, the values of V and W were evaluated, and from the best-fit value of W the average K -nucleon cross section was determined.

The fundamental K -nucleon interactions which have been assumed are those predicted by the scheme of Pais,⁶ Gell-Mann,⁷ and Nakano and Nishijima.⁸ They may be written as follows:

$$K^+ + p \rightarrow K^+ + p, \quad (1)$$

$$K^+ + n \rightarrow K^+ + n, \quad (2)$$

$$K^+ + n \rightarrow K^0 + p, \quad (3)$$

where K^+ and K^0 are the two charge states of the K meson (strangeness=1, isotopic spin= $\frac{1}{2}$, and spin=0) and where n and p represent neutron and proton.

Under the assumption of the independent-particle model of the nucleus, and from experimentally determined K -hydrogen,⁹ inelastic K -nucleus, and K -nucleus charge-exchange cross sections, the total cross sections for reactions (2) and (3) were obtained.

Reaction (1) occurs in isotopic spin state $T=1$ and reactions (2) and (3) occur in isotopic spin states $T=1$ and $T=0$. If we assume S - and P -wave scattering only, the three processes may be described by six phase shifts corresponding to six scattering amplitudes. The total cross section for the above reactions and the nuclear potential V are related to these phase shifts. Using these relations and the available experimental data, values for the phase shifts were obtained. From these values, the differential scattering cross sections for the above reactions have been estimated.

⁶ A. Pais, *Physica* **19**, 869 (1953).

⁷ M. Gell-Mann, *Phys. Rev.* **92**, 833 (1953).

⁸ T. Nakano and K. Nishijima, *Progr. Theoret. Phys. (Japan)* **10**, 581 (1953).

⁹ T. F. Kycia, L. I. Kerth, and R. G. Baender, *Bull. Am. Phys. Soc.* **4**, 25 (1959), and *Phys. Rev.* **118**, 553 (1960); T. F. Kycia, thesis, University of California Radiation Laboratory Report UCRL-8653 (unpublished).

* This work was performed under the auspices of the U. S. Atomic Energy Commission.

¹ The initial results from this investigation were reported in a Letter to the *Phys. Rev.* **108**, 1098 (1957), and in the *1958 Annual International Conference on High-Energy Physics at CERN*, edited by B. Ferretti (CERN Scientific Information Service, Geneva, 1958), in which all the available data were summarized by M. F. Kaplon, pp. 171–175.

² D. Keefe, A. Kernan, A. Montwill, M. Grilli, L. Guerriero, and G. A. Salandin, *Nuovo cimento* **12**, 241 (1959). In this paper, references to previous emulsion data at lower energies are given.

³ D. H. Stork, *Proceedings of the International Conference on the Nuclear Optical Model, The Florida State University Studies, No. 32*, edited by A. E. S. Green (The Florida State University, Tallahassee, 1959).

⁴ O. R. Price, D. H. Stork, and I. I. Rabi, *Phys. Rev. Letters* **1**, 212 (1958); D. Fornet Davis, N. Kwak, and M. F. Kaplon, *Phys. Rev.* **117**, 846 (1960).

⁵ S. Fernbach, R. Serber, and T. B. Taylor, *Phys. Rev.* **75**, 1352 (1949).

TABLE I. Details on separated beams.

Incident K^+ -meson momentum (Mev/c)			Total length (cm)										
1	2	3	4	5	6	7	8	9	10	11	12	13	14
Expected	Experimentally determined ^a	Momentum spread ^b	Accelerator	Target length in beam direction (cm)	Target material	Angle of K^+ beam to proton beam	Estimated effective solid angle of acceptance ^c	First system	Second system	Length of beryllium degrader	Exposure in No. of protons on target	K^+ mesons per mm of 400- μ plate (averaged over 2 in.)	Average ratio min tracks to K^+ tracks
520	515	± 25	Cosmo	7.5	Cu	35°	0.0005	320	320	5	1×10^{13}	1.3	35
625	622	± 12	Beva	3.2	Cu	53°	0.001	568	626	67	8×10^{13}	0.9	3
700	720	± 14	Beva	3.2	Cu	53°	0.001	568	626	58	1×10^{14}	1.9	9

^a Best estimate of the average incident K -meson momentum.

^b Calculated from magnet dispersion in experimental arrangement. The values determined from the K range distribution were ± 15 Mev/c for the 622-Mev/c stack and ± 20 Mev/c for the 720-Mev/c stack. A less accurate value for the 515-Mev/c stack was $\sim \pm 26$ Mev/c (see text).

^c In making this estimate no account was taken of losses in the degrader due to inelastic K -nucleus scattering or to wide-angle elastic scattering.

Multiple collisions of the K mesons with nucleons occur in emulsion nuclei, and it is for this reason that a Monte-Carlo cascade calculation was performed. The results of the calculation compared quite well with the experimental data but were found to be insensitive even to gross changes in the K -neutron center-of-mass angular distributions. The method was useful in estimating the number of inelastic scatterings that were misclassified as elastic. It also served as a means of determining the effect of multiple K -nucleon collisions in nuclei on the observed relative number of charge-exchange events.

In addition to the interactions (1), (2), and (3), given the high energy of the incident K particles, π -meson production is possible, and it is not in discord with the above-mentioned theoretical schemes. The reactions predicted would be similar to those above, but with a π meson of appropriate charge as an additional reaction product. A total of three examples of π production have, thus far, been reported; one of these was observed in this experiment. From the combined data and from a Monte-Carlo phase-space calculation, an estimate of the cross section for charged-pion production in K^+ -nucleon encounters has been obtained.

The possibility that interactions exist which might violate the scheme of Pais, Gell-Mann, and Nakano and Nishijima has been carefully considered during the analysis of each event. No evidence has been found to affirm their existence.

II. EXPERIMENTAL

A. Exposures

In this experiment three pellicle stacks of nuclear emulsion were exposed in "separated" beams using two experimental arrangements. The one illustrated in Fig. 1 was designed with Dr. D. Meyer and used at the Cosmotron to expose at a final K -particle momentum of 515 Mev/c. The other system was designed by Dr. D. H. Stork and Dr. J. H. Mulvey and used at the

Berkeley Bevatron to expose at 622 Mev/c and 720 Mev/c K -particle momentum.

The details of these systems and the resultant beams are given in Table I.

The average momentum and momentum spread as calculated from the geometry of the experimental arrangement are listed in columns 1 and 3 of Table I. The momenta have also been determined from measurements made in the emulsions stacks exposed.

In the two exposures at 622 and 720 Mev/c, auxiliary stacks were placed to the rear of the main stacks to bring the K^+ mesons to rest. From the range distribution of K^+ mesons entering in a two-inch length along the leading edge of these stacks and within a 20° cone, an average range of the K mesons incident on the main stack was determined. The corresponding average momenta were taken from the range-momentum curves of Atkinson and Willis.¹⁰ The histograms for these range distributions appear in Fig. 2. The values so obtained, believed to be the most accurate determination of the average incident momentum, are listed in column 2 of Table I.

The incident momentum may also be determined in the same stack in which the K interactions are studied:

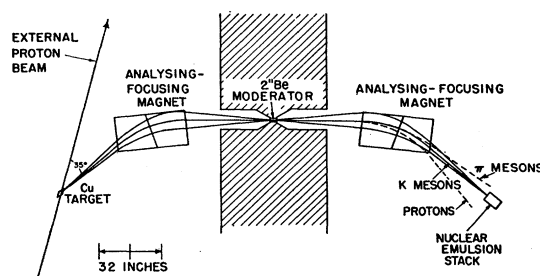


FIG. 1. Experimental arrangement for nuclear-emulsion exposure at Cosmotron.

¹⁰ J. H. Atkinson and B. H. Willis, University of California Radiation Laboratory Report UCRL-2426, 1957 (unpublished), Vol. II.

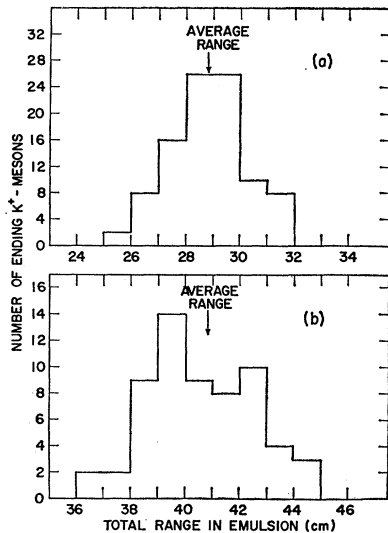


FIG. 2. Range distribution in nuclear emulsion for incident K^+ mesons: (a) 622-Mev/c exposure, (b) 720-Mev/c exposure.

(a) from multiple-scattering measurements on the K tracks near the leading edge of the stack, (b) from determination of the specific ionization by normalized grain counts on incident K -particle tracks.

Both methods were employed in the determination of the incident K momentum for the stack exposed at the lowest momentum. The momentum distributions obtained from these methods appear in Fig. 3. As no K -range determination was provided for in this exposure, the value determined from Fig. 3 was taken as the average incident- K momentum. The value is listed in column 2 of Table I.

The momentum spread of the K beam, which was previously calculated from the dispersion in the magnet systems and from the degrader size, may be checked using the observations on K ranges and subtracting out the effect of range straggling. The value obtained for the stack exposed at 622 Mev/c is ± 15 Mev/c and for the 720-Mev/c stack is ± 20 Mev/c. Both figures are larger by 20–30% than the values given in Table I, indicating the existence of an additional spread in momentum possibly produced by the long degrader. The momentum spread for the 515-Mev/c stack was evaluated from the distributions of Fig. 3(b). It was found to be $\sim \pm 26$ Mev/c which is in good agreement with the value listed in Table I.

B. Stack Preparation and Scanning

The three stacks used were composed of Ilford G5 pellicles 400μ thick. The stack dimensions were enlarged as the incident momentum increased. For the 515-Mev/c exposure 36 pellicles 3 in. \times 4 in. were used, for the 622-Mev/c exposure 108 4-in. \times 8-in. pellicles were used, and for the 720-Mev/c exposure 136 4-in. \times 8-in. pellicles were used. For ease in scanning, the stacks were

exposed so that the incident K beam was parallel (within 1°) to the emulsion plane and also approximately perpendicular to the leading edge of the stack. Following exposure, the stacks were disassembled and on each emulsion a coordinate grid was printed on the surface which was to be placed in contact with the glass plate. The pellicles were then mounted on glass and processed using BNL's standard technique.¹¹

Scanning for K tracks was then begun along the leading edge of each plate and at a distance of 2 mm from the edge for the 515-Mev/c stack and 8 mm from the edge for the 622-Mev/c and 720-Mev/c stacks. As K tracks had an ionization of 1.25–1.45 times the minimum value, and as the background tracks were either denser or lighter, the scanning consisted in selecting beam tracks in the appropriate grain-density region. To reduce to a minimum the number of background tracks selected, a grain count on each track of ~ 300 grains was made. If the count lay within the expected limits, track following and scanning along this K track was begun. If possible, this was continued to near the trailing edge of the stack, i.e., a total of 9 cm in the 515-Mev/c stack and of 18 cm in the 622- and 720-Mev/c stacks. At this point, and also when the track was abandoned¹² or an interaction or decay occurred, a new grain count of ~ 300 grains was made, and this value also had to lie within the limits expected for a K meson.

During the tracing of tracks through the stacks the following events were recorded:

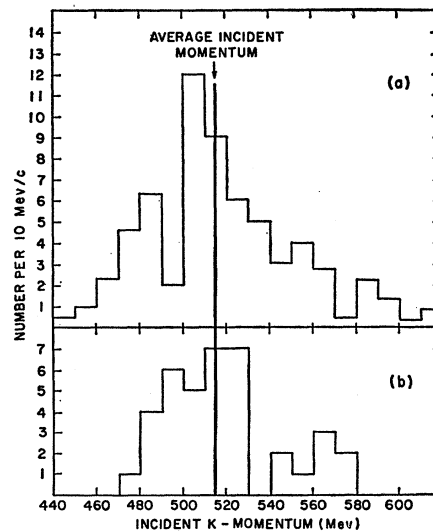


FIG. 3. Momentum distribution for incident K^+ mesons in 515-Mev/c exposure: (a) from multiple scattering measurements, (b) from ionization (g/g_0) measurements.

¹¹ J. F. Garfield, Phot. Sci. Eng. 2, 85 (1958).

¹² To increase the track-scanning speed, the track was abandoned if its projected length in a single emulsion became less than 2 mm for the 515-Mev/c stack and 5 mm for the 622- and 720-Mev/c stacks.

(a) Abrupt deviations or single scatterings of projected angle $\geq 1.5^\circ$. (This limit was increased to $\geq 2^\circ$ in the scanning of the 515-Mev/ c stack.) These events were preliminary classified as elastic scatterings unless either a noticeable increase in grain density was seen, or the event was accompanied by other ionizing tracks (including low-energy electrons and/or blobs); in such cases it was classified as inelastic.

(b) Cases in which there was a noticeable reduction in grain density of the track, usually accompanied by a change in projected angle. These were tentatively called decays in flight.

(c) Events not classifiable as elastic scatterings or decays in flight, which were called inelastic events.

On observation of an event it was classified as indicated above, and a drawing and the measurements of projected and dip angles of all tracks in the event were made and their values recorded.

C. Analysis

In order to classify events as (a) elastic scattering, (b) inelastic scattering with secondary K^+ meson, (c) inelastic scattering with no visible K meson (assumed to be charge exchange),¹³ (d) decays in flight, and (e) K -hydrogen scatterings, an accurate analysis of each event was required. The analysis consisted in the identification of charged particles and in the determination of the range in emulsion or of the velocity at emission of secondary charged particles.

During this analysis, all events were again carefully scrutinized for missing tracks and all drawings and previous measurements checked.

The methods used in track analysis were, in all cases but one, standard emulsion techniques. Therefore, these will only be summarily mentioned, the exception being dealt with in slightly greater detail.

Secondary particles leaving the emulsion stack before coming to rest were usually identified by observing the variation in specific ionization along the track as determined by the normalized grain count g/g_0 where g_0 is the average grain density of minimum tracks near the track of interest. In each measurement at least 600 grains along the track and 1200 grains along minimum tracks at the same depth in the emulsion were counted. The g/g_0 vs range curves for the three emulsion stacks with relative calibration points are displayed in Fig. 4. Although the calibration utilized tracks of pions, muons, protons, and K^+ mesons, all points were transformed so as to correspond to particles having a K -meson mass.¹⁴

Another standard method that may be utilized for mass determination of nonending particles is multiple

¹³ The fact that these events are indeed charge-exchange events has been demonstrated in a recent counter experiment: M. N. Whitehead, R. E. Lanou, Jr., V. Cook, Jr., and R. Birge, *Phys. Rev.* **118**, 300 (1960).

¹⁴ The K^+ -meson rest mass used in the construction of these curves was 494.0 Mev. This value of the K^+ mass was assumed throughout.

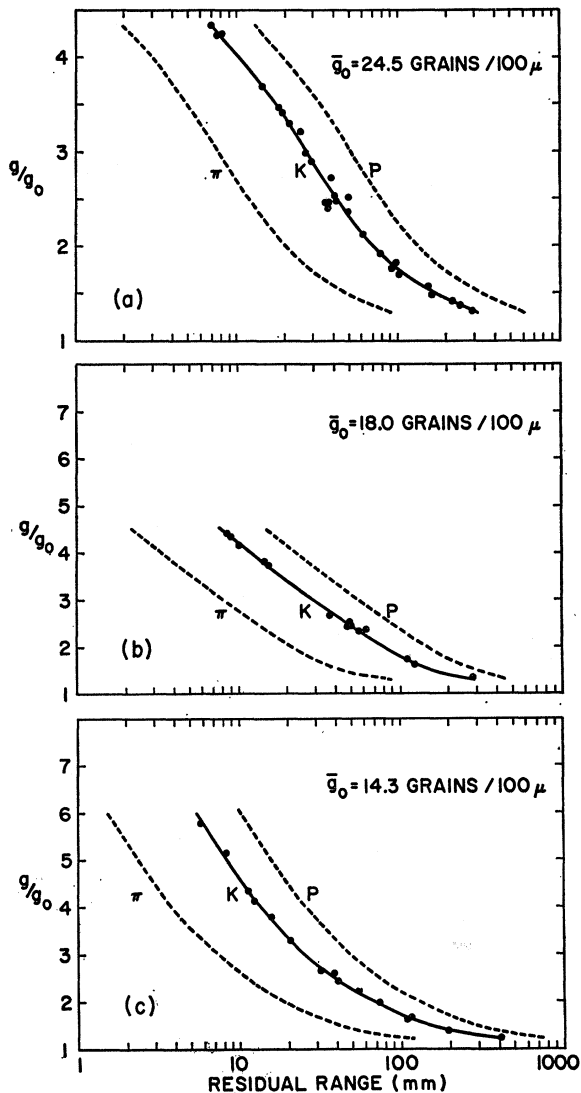


FIG. 4. Calibration curves for specific ionization-range measurement: (a) for 515-Mev/ c stack, (b) for 622-Mev/ c stack, (c) for 720/ c stack; calibration points referred to K -meson mass. The average minimum grain density \bar{g}_0 is also given.

scattering vs g/g_0 measurement. This method was principally applied in determining the purity of the K beam selected by the scanners.

Unstable particles ending in the emulsion stacks may be identified quite simply by observing their decay products, thus distinguishing K^+ and π^+ mesons from protons. To use this as a means of identification, one must observe the decay products, which are often at minimum, with high efficiency. This was not found to be possible in all stacks used in this investigation. We were, in fact, able to apply this criterion convincingly only in the 515-Mev/ c stack where the minimum grain density was 24.5/100 μ , where the background was low, and where the observation of minimum tracks was therefore quite efficient.

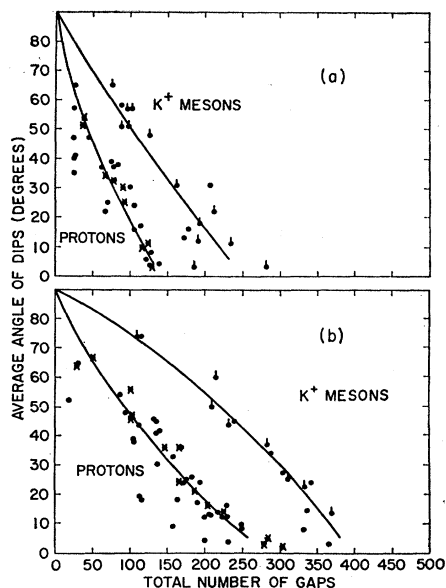


FIG. 5. Integral number of gaps with projected length $\geq 0.4 \mu$ in a projected range from 200 to 1500 μ , plotted vs average dip angle in 400- μ thick emulsion: (a) for 622-Mev/c stack, (b) for 720-Mev/c stack. Measurements on tracks which were identified by this method are indicated by \bullet without additional marking. Calibration points are marked by \times for protons and \downarrow for K^+ mesons.

In the 622-Mev/c and 720-Mev/c stacks the background was high and the minimum low (see Fig. 4), and thus for these stacks another method of identification for stopping particles was necessary. The integral gap-count method was used but was modified to permit greater speed in application.¹⁵ It consisted in the determination of the integral number of gaps of projected length $\geq 0.4 \mu$ over a projected length of the track beginning at 200 μ and extending to 1500 μ from the end of the range. The average dip of the track in degrees (referred to the original thickness of the emulsion) was also determined. The identity of the particle was established from a plot of this average dip vs the integral gap count. These plots are presented in Fig. 5. The average curves for K and proton are indicated together with the measured points.

As is evident from the curves, a single calibration in a stack, without normalization, is sufficient to identify tracks as K^+ mesons or protons¹⁶ unless the average dip angle is less than 5° or greater than 80° . The method is most satisfactory for low levels of grain density as is the case for the 720-Mev/c stack (minimum grain density ~ 14 grains/100 μ). For very flat or very steep tracks (and for a few doubtful events of the 515-Mev/c stack)

¹⁵ The modification on the standard gap-counting method was suggested by Mr. J. Greener.

¹⁶ A satisfactory distinction between K^+ meson and proton could still be made with measurements on 800 μ projected range, but the statistical errors were larger as the total number of gaps in each track was decreased by a factor ~ 2 .

a direct comparison of gap counts with those of known particles in the same area of the emulsion was made.

Using these methods of particle identification, it was found possible to identify almost all secondary particles having ranges ≥ 2 mm. In a few doubtful cases (~ 10), in which track identification was difficult due to shortness of tracks leaving the emulsion or to irregularities in the emulsion, it was necessary to use "reasonableness" arguments based on the assumption that K mesons are scattered in nuclear matter but not absorbed. These events may not be taken as evidence for or against the reaction schemes theoretically predicted.

To classify events properly, a distinction must be made between elastic scatterings and those inelastic scatterings in which the K meson loses a small amount of energy (≤ 60 Mev) but produces no visible nuclear disintegration. Using the most sensitive measure of change of energy or velocity, i.e., a change in the g/g_0 of the track of the particle after the scattering, and selecting those so-called "elastic" events whose scattering angle was large and thus most probably inelastic¹⁷ ($\geq 15^\circ$ in the 515-Mev/c stack and $\geq 10^\circ$ in the 622- and 720-Mev/c stacks), a search for inelastic events was made. The number of misclassified events that were found in this search was small. A rough estimate of the percentage of energy loss detectable in this way was 8% for the 515-Mev/c stack, 10% for the 622-Mev/c stack, and 12% for the 720-Mev/c stack. The further correction to the results for events with undetectable loss of energy will be discussed in a later section where the experimental results are compared with a Monte-Carlo cascade calculation.

K -hydrogen scattering events could be identified with high efficiency because of their unique kinematics. Their identity was established by determinations of angles, complanarity, and energies.

With the aforementioned limitations we may now classify the events in the four categories previously indicated. A summary for each stack appears in Table II.

In criticizing these results, one may in general question the efficiencies of observation. For elastic scatterings we have evaluated the observational inefficiencies in various angular intervals for each observer in each stack by a rescanning technique. The efficiencies were found to be as small as $\sim 50\%$ in the projected angular interval $2-3^\circ$ and quite high at large angles, but strongly observer dependent.¹⁸ The results given later have been corrected for these scanning biases, whereas the results in Table II have not.

¹⁷ Inelastic scattering is unlikely at small angles (where the Coulomb scattering is significant), (a) because the solid angle is small, and (b) because the Pauli principle is most effective in reducing the cross section at small angles where the momentum transfer is small.

¹⁸ For scattering angles less than 4° , uncertainties in the correction may possibly have affected the results by $\sim 10\%$. At larger angles the corrections are small and the uncertainties negligible.

TABLE II. Experimental results for each emulsion stack.

Stack	515 Mev/c	622 Mev/c	720 Mev/c
Length of K track followed, m	122	70	94
Elastic scatterings ^a	465 ^b	325 ^c	183
Decays in flight	44	14	20 ^d
K -meson lifetime from decay in flight, sec ^e	$(1.03 \pm 0.15)10^{-8}$	$(1.5 \pm 0.4)10^{-8}$	$(1.20 \pm 0.27)10^{-8}$
Noncharge-exchange inelastic scatterings	161	139	173
Charge-exchange scatterings	38	44	72
K -hydrogen scatterings ^f	6	5	4
K -hydrogen cross section, mb		$16.5_{-6.5}^{+3.5}$	

^a These are observed values which have not been corrected for scanning biases due to limiting cutoff angle in observation or for observational inefficiencies.

^b This value refers to observations made on 105.5 M of track.

^c This value refers to observations made on 63.5 M of track.

^d This number includes three stops in flight which were classified as decays in which the secondary particles could not be detected.

^e From the total number of decays in flight and the total proper time of flight, the mean lifetime of the K^+ meson was calculated to be $(1.15 \pm 0.13)10^{-8}$ sec. From measurements made by counter technique,¹⁹ the mean life is $(1.224 \pm 0.013)10^{-8}$ sec.

^f The K energies in the laboratory system and the center-of-mass scattering angles of each event are,

for the 515 Mev/c stack: 194 Mev, 146°; 188 Mev, 95°; 176 Mev, 92°; 168 Mev, 104°; 155 Mev, 80°; 153 Mev, 98°;

for the 622 Mev/c stack: 290 Mev, 116°; 285 Mev, 119°; 285 Mev, 78°; 280 Mev, 81°; 213 Mev, 12°;

for the 720 Mev/c stack: 330 Mev, 164°; 291 Mev, 173°; 283 Mev, 126°; 256 Mev, 133°.

The efficiencies of detection of particle tracks with low grain densities may influence the results. This becomes more important as the minimum grain count becomes smaller and as the K particle approaches the minimum in specific ionization. The 720-Mev/c stack was particularly susceptible to this effect ($\bar{g}_0 = 14.3$ grains/100 μ), and partially, also the 622-Mev/c stack ($\bar{g}_0 = 18.0$ grains/100 μ). In both stacks, but in particular in the 720-Mev/c stack, an intense effort was made to reduce losses to a bare minimum. Events were in fact carefully scrutinized at least two times by different observers.

D. Purity of K^+ Beam

The reliability of our results is also directly related to the purity of the beam selected by the scanners. Although the mean lifetime for decay in flight for beam particles was consistent with the K^+ -meson mean life of $(1.224 \pm 0.013)10^{-8}$ sec.¹⁹ and although a large number of K mesons were identified as secondaries in the study of stars produced, the primary beam as selected could still have contaminants in the form of π mesons, μ mesons, or protons. For those tracks which were followed to near the trailing edge of the stack, the variation of grain count over this long range identified the particle. Particles that interacted in flight or that were followed only a few centimeters could be identified from g/g_0 and multiple-scattering measurements. Primaries of all charge-exchange events were analyzed in this way.

Only two protons and three π and μ mesons were detected, and it is believed that the remaining beam was virtually devoid of contaminants.

E. Results

In Table II the results were presented separately for each stack. To study the dependence on energy of the

K -meson cross sections, the data have been divided into three K -meson energy intervals. These data are presented in Table III where the values given were corrected both for losses due to inefficiencies of observation and for geometrical losses. The most noticeable feature of these results is that the total inelastic cross section, the charge-exchange cross section, and the charge-exchange/noncharge-exchange ratio all increase with increasing K energy.

Experimental determination of the elastic K -nucleus differential cross section for the three energy intervals has been made. The results are presented in Fig. 7 where they are compared with an optical-model calculation.

 TABLE III. Experimental results for three K^+ energy intervals.

Energy interval, Mev	142–218	218–295	295–373
Average energy \bar{T}_K , Mev	189	257	334
K^+ -track length followed, m	128.2	85.7	71.2
Elastic scatterings $\geq 2^\circ$ ^a	781 ^b	350 ^c	204
Cross section per emulsion nucleus for elastic scattering $> 4^\circ$, mb ^a	633 ± 43 ^b	400 ± 37 ^c	243 ± 31
Cross section per emulsion nucleus for elastic scattering $> 6^\circ$, mb ^a	335 ± 29 ^b	224 ± 28 ^c	128 ± 21
Inelastic scatterings (C.E. and Non C.E.)	215	166	136
Cross section per emulsion nucleus for inelastic scattering, mb	358 ± 25	413 ± 33	407 ± 35
Charge-exchange scatterings	42	56	56
Cross section per emulsion nucleus for charge-exchange scattering, mb	70 ± 11	139 ± 18	167 ± 24
Charge-exchange/noncharge-exchange π meson produced	0.24 ± 0.04	0.51 ± 0.08	0.70 ± 0.12

^a Corrected for geometrical losses and inefficiencies in observations of elastic events.

^b This value refers to observations made on 105.5 m of track in this energy interval.

^c This value refers to observations made on 79.2 m of track in this energy interval.

¹⁹ See p. 85 of reference 10.

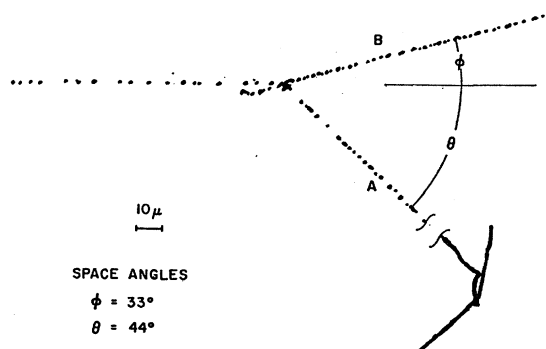


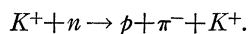
FIG. 6. Drawing of event in which π^- meson was produced by K^+ meson. Track B was produced by the secondary K^+ meson, track A by the π^- meson.

The angular and energy distributions for secondary K^+ mesons and energetic protons ($T_p \geq 40$ Mev) from inelastic events were also determined for the three energy intervals. They are presented in Figs. 8 and 9 where they have been compared with the results of a Monte-Carlo cascade calculation.

F. π^- -Meson Production Event

A single example of a π^- meson produced by a K^+ meson was observed. A drawing of this event is shown in Fig. 6. The primary was identified as a K particle by ionization and multiple-scattering measurements on 2.4 cm of track in the plate in which the event occurred. The energy of the K at the interaction was 280 Mev. The secondary particle causing track A came to rest in the stack after 6.8 mm, producing a characteristic π^- capture star of 2 black prongs and a recoil track. Ionization-range measurements further confirmed this identification. The π^- energy at emission was 19 Mev. The particle producing track B left the stack after 1.7 cm and was identified as a K meson by variation of ionization with range and by ionization-multiple-scattering measurements. Its energy at the interaction was 96 Mev. The event is further characterized by a blob and a slow electron appearing to originate at the star center.

This event may be interpreted according to the following scheme:



Considering this reaction as valid, the energy given to the proton in the nucleus was found to be 26 Mev (corresponding momentum 360 Mev/c).

The proton is not observed, but the presence of a blob or recoil would indicate a nuclear excitation consistent with the 26-Mev unbalance in energy. Considering only the primary and the two visible secondaries, the unbalance in momentum is 318 Mev/c. This value is consistent with the above interpretation and further indicates that the K and π mesons left the nucleus without appreciable loss of energy.

III. DISCUSSION

The optical model of the nucleus has been adopted in the study of the K -nucleus interaction. The K^+ meson is assumed to be scattered by the Coulomb potential V_c and by a complex nuclear potential of the form suggested by Wood and Saxon²⁰:

$$\frac{V+iW}{1+\exp[(r-r_0)/d]}$$

The elastic K -nucleus scattering calculated assuming this model is principally determined by V and V_c . From a comparison of the observed elastic cross section with those calculated for various values of V , the magnitude of V and its sign relative to V_c can be evaluated. Due to some uncertainty as to the classification of elastic events, a comparison of the integral elastic plus total inelastic cross section with that calculated has been used to give the most reliable estimate of the magnitude of V . The value of W is obtained by comparison of the experimental inelastic K -nucleus cross section with those calculated. The inelastic cross section is considered to result from K -nucleon scattering in the nucleus; therefore, the K -nucleon cross section in nuclear matter, $\bar{\sigma}_W$, may be deduced from a knowledge of W . The "free" K -nucleon cross section has been obtained from $\bar{\sigma}_W$ after correcting for the effect of the Pauli principle.

Under the assumption of the independent-particle model of the nucleus, the values of the cross section for K -neutron scattering can be deduced. This has been done by subtracting from the average K -nucleon cross section the properly weighted K -proton cross section. The partial cross sections for the two modes of K -neutron scattering, reactions (2) and (3), have been evaluated from the total K -neutron section and from a knowledge of the relative number of charge-exchange events.

Corrections to the previous results were necessary in order to account for the misclassification of inelastic events as elastic and for the effect of multiple collisions and of the Pauli principle on the relative number of charge-exchange events. These corrections have been estimated by a Monte-Carlo cascade calculation.

Assuming S - and P -wave scattering only, the total cross sections for the three reactions (1), (2), and (3), as well as the real nuclear potential V , may be expressed in terms of six phase shifts. A search for the phase shifts that give the experimentally observed cross sections and the real nuclear potential has been made. The phase shifts that were determined in this way have been used to predict the form of the K -neutron differential scattering cross sections.

A. Optical-Model Calculation

The K^+ -nucleus interaction was investigated by an optical-model calculation.⁵ Using the Coulomb poten-

²⁰ R. D. Wood and D. S. Saxon, Phys. Rev. **95**, 577 (1954).

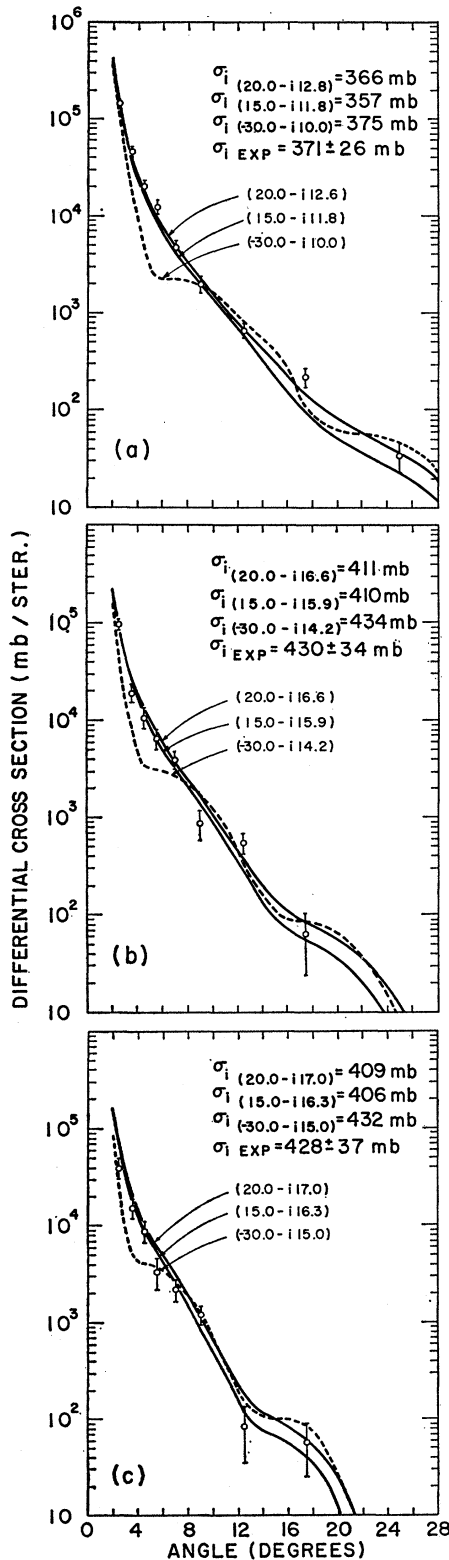


FIG. 7. K^+ -nucleus differential cross section for elastic scattering plotted vs the laboratory scattering angle. Curves from an optical model calculation with varying values of $V+iW$ are

tial and a Wood-Saxon nuclear potential with $r_0 = 1.15A^{1/3} \text{ f}$ and $d=0.57 \text{ f}$, the calculation was made by the evaluation, by partial waves, of the Schrödinger wave equation corrected for relativistic effects²¹ (see Appendix). The differential elastic and the total inelastic cross sections for a particular element and for particular values of the incident K energy and of the real and imaginary nuclear potentials were in this way evaluated.²² In this calculation, nuclear emulsion was assumed to be composed of Ag, Br, and N nuclei, with percentage concentrations of 22%, 22%, and 56%, respectively. These percentages were applied as weighting factors to the resultant cross sections for each element in order to calculate the average elastic differential and total inelastic cross sections.

The computer program used was written by Dr. G. Igo for an IBM 704 computer, and was applied previously in a study of K^+ -nucleus scattering at lower energies.²³

Assuming various values for V and choosing W so as to obtain an inelastic cross section close to that experimentally observed, a number of curves for differential elastic scattering were calculated. A set of three of these for each energy interval are shown in Figs. 7(a), 7(b), and 7(c), where they are compared with the experimentally determined elastic differential cross sections. The calculated total inelastic cross sections are also given in each figure. As the calculated elastic scattering was found to be sensitive to changes in V only and the inelastic cross section only to changes in W , V and W have been calculated separately, and the results corrected for correlations in the values. The best-fit values of V and W for the three energy intervals are given in Table IV (columns 2 and 3).

The best-fit values for V indicate a positive (repulsive) K -nuclear potential at all three energies. This fact is most clearly demonstrated in the results for the lowest energy interval. Qualitatively, this can be seen from the poor fit of the experimental points to the curves for negative V shown in Figs. 7(a), 7(b), and 7(c).²⁴

An alternative method for determining the magnitude of the real nuclear potential, V , was employed by Igo *et al.*²³ The method relates the total cross section, for inelastic scattering plus that for elastic scattering at

²¹ In this evaluation, phase shifts for values of l up to 25 were calculated.

²² The optical model potentials were taken as proportional to ρ_0 , [note Eq. (10) of Sec. IIIC]. The values of V and W which are quoted refer to the average value for Ag and Br ($\rho_0=0.139 \text{ f}^{-3}$).

²³ G. Igo, D. G. Ravenhall, J. J. Tieman, W. W. Chupp, G. Goldhaber, S. Goldhaber, J. E. Lannutti, and R. M. Thaler, Phys. Rev. **109**, 2133 (1958).

shown along with experimentally determined cross sections. Corresponding values of the total inelastic cross section together with the observed values are also listed. The calculations and experimental results refer to three average K energies, (a) 189 Mev, (b) 257 Mev, and (c) 334 Mev.

²⁴ The figures show curves for $V=-30.0 \text{ Mev}$. For $V=-15.0 \text{ Mev}$ and even poorer fit to the data results.

TABLE IV. K -nucleus optical-model potentials.

1	2	3	4	5	6
Average kinetic energy \bar{T}_K (Mev)	Real nuclear potential V from elastic scattering (Mev)	Imaginary nuclear potential W (Mev)	Limiting angle for elastic scattering $\theta > 6^\circ$ (Mev)	Limiting angle for elastic scattering $\theta > 4^\circ$ (Mev)	Corrected imaginary nuclear potential W (Mev)
189	21.2±3.0 ^a	-12.8±1.4	18.0±3.6 ^a	18.0±3.3 ^a	-12.9±1.4
257	20.3±3.1	-16.5±2.0	19.5±4.0	18.5±3.6	-17.4±2.0
334	15.7±3.2	-16.1±2.5	16.5±6.5	13.5±5.0	-17.6±2.5

^a The error in this value has been increased by 1 Mev to take into account possible imprecision in the determination of the average K energy.

angles greater than a certain limiting angle, to the nuclear potential V . The advantage of this method is clear, for it eliminates the difficulty of making a sharp distinction between elastic and inelastic scattering. The total cross sections were calculated, for limiting angles for elastic scattering of 4 and 6 degrees. From a comparison of experimental results with those calculated, values of V were obtained. These are given in Table IV, columns 4 and 5. The values of V for a limiting angle for elastic scattering of 8 degrees were also determined and were found to agree closely with the values for 6 degrees. The most reliable estimates of the magnitude of V are considered to be the results obtained for a limiting angle of 4 degrees. The sign of the potential as deduced from the differential cross section for elastic scattering is positive.

The misclassification of inelastic events as elastic may be taken into account in the determination of V as explained above, but the values of W as determined from the number of inelastic events are systematically affected. The correction to the number of inelastic events was obtained from a comparison of the K -energy loss distribution which was observed, with those obtained from the Monte-Carlo cascade calculation (discussed in Sec. IIID). The number of events found to have been missed in the search for inelastic events was 8 ± 2^{25} in the lowest energy interval $\bar{T}_K = 189$ Mev, 7 ± 3^{25} in the central energy interval $\bar{T}_K = 257$ Mev, and 7 ± 2^{25} in the highest energy interval $\bar{T}_K = 334$ Mev. The effect on W due to the inclusion of these events is small. The corrected values have been listed in the last column of Table IV.

The values of V and W which have been determined refer to scattering by a Wood-Saxon potential with $r_0 = 1.15A^{1/3}$ f and $d = 0.57$ f. This value of r_0 is intermediate between $1.07A^{1/3}$ f and $1.20A^{1/3}$ f which represents a reasonable range for variation for K scattering. Had other values of r_0 and d been chosen, different values of the potentials V and W would have been obtained. This has been investigated for K^+ scattering in emulsion by the University of California at Los

²⁵ The errors in these values refer to the resultant variation when the K -neutron differential scattering cross sections are changed from predominantly forward to predominantly backward.

Angeles.³ At 261-Mev K^+ energy they report values for $V+iW$ of $(14 \pm 5) - i(11.7 \pm 1.5)$ Mev for $r_0 = 1.20A^{1/3}$ f and $d = 0.57$ f, and $(22 \pm 6) - i(19.3 \pm 2.0)$ Mev for $r_0 = 1.07A^{1/3}$ f and $d = 0.57$ f.

These results of the UCLA group may be compared with our results for the central energy interval ($\bar{T}_K = 257$ Mev), of $(18.5 \pm 3.6) - i(17.4 \pm 2.0)$ Mev. Taking into account the values of r_0 and d which were assumed, the results are found to agree within the errors.

B. K -Nucleon Cross Sections

Assuming an independent-particle model of the nucleus in which inelastic nuclear encounters are represented as K -nucleon interactions in the nucleus,²⁶ we may now, in the framework of the optical model, determine the K -nucleon cross section. The imaginary nuclear potential, W , is proportional to the imaginary part of the K -nucleon forward scattering amplitude, $\text{Im}[\hat{f}(0)]$. $\text{Im}[\hat{f}(0)]$ is in turn proportional to the average K -nucleon cross section $\bar{\sigma}_W$ [see Eqs. (9) and (10), Sec. IIIC] and thus $\bar{\sigma}_W$ may be expressed in terms of W . The relation may be written as follows:

$$\bar{\sigma}_W = 2WE_K/\hbar c^2 p_K \rho_0,$$

where $\rho_0 = 3A/[4\pi r_0^3(1 + \pi^2 d^2/r_0^2)] = 0.139f^{-3}$, and where E_K and p_K are the total energy and momentum of the K particle in the nucleus. The values of $\bar{\sigma}_W$ calculated for the three energy intervals are listed in Table V (column 4).

An alternative determination of this value was made using the methods of Cronin, Cool, and Abashian²⁷ who calculated the nuclear transparency assuming undeviated trajectories through the nucleus. This calculation, however, does not take into account the effect of the Coulomb field in deviating the trajectories of the particles before their arrival at the nuclear boundary. This was corrected for, using a relation derived by Sternheimer.²⁸ The values of the K -nucleon cross section, $\bar{\sigma}$,

²⁶ This follows from the fact that the deBroglie wavelength of the K^+ mesons in the energy range of this experiment is ~ 0.6 f and that the average nuclear spacing in the nucleus is ~ 1.4 f.

²⁷ J. W. Cronin, R. L. Cool, and A. Abashian, Phys. Rev. **106**, 1027 (1957).

²⁸ R. M. Sternheimer, Phys. Rev. **101**, 384 (1956).

TABLE V. K -nucleon total cross sections.

1	2	3	4	5	6	7	8	9
Average kinetic energy (Mev)	Average kinetic energy in nucleus (Mev)	Effective K -nucleon cross section $\bar{\sigma}$ (mb)	Effective K -nucleon cross section from imaginary potential W $\bar{\sigma}_W$ (mb)	Pauli-principle corrected cross section $\bar{\sigma}_{ub}$ (mb)	Corrected C.E./non C.E. ratio f_c	K -proton cross section ^a σ_{Kp^+} (mb)	K -neutron scattering cross section σ_{Kn^+} (mb)	K -neutron charge-exchange cross section σ_{Kn^0} (mb)
189	165	13.7±1.5	14.1±1.5	16.0±1.8	0.19±0.03	15.0	12.1±1.6	4.6±1.2 ^b
257	233	17.2±2.1	17.3±2.1	18.9±2.2	0.38±0.06	15.5	10.5±1.8	9.3±2.2 ^b
334	315	16.7±2.0	16.2±2.0	17.3±2.1	0.50±0.08	16.0	8.0±1.5	10.3±2.4

^a Results taken from summary of world data on $K-p$ scattering prepared by L. Kerth, presented by L. Alvarez at the High-Energy Conference held at Dubna, Russia, 1958 (unpublished). The values listed were taken from a best-fit curve to the experimental points. The error in each was estimated to be ±0.5 mb.

^b Within the errors these values agree with those recently obtained in a counter experiment¹² on charge-exchange scattering in the K energy interval 175-250 Mev.

obtained in this way are also presented in Table V (column 3). These values agree within 1 mb with the values of $\bar{\sigma}_W$.

$\bar{\sigma}_W$ (and $\bar{\sigma}$) refers to an effective cross section in nuclear matter where the Pauli principle is operative. The cross sections for unbound nucleons, $\bar{\sigma}_{ub}$, were obtained by applying a correction, derived by Sternheimer,²⁹ for the effect of the Pauli principle. In its derivation a momentum distribution for the nucleons in a nucleus of the form $p_F^2 d p_F$ and an isotropic center-of-mass K -nucleon angular distribution have been assumed. The expression for the corrected cross section is³⁰:

$$\bar{\sigma}_{ub} = \bar{\sigma}_W (1 - RT_F/T_K)^{-1},$$

where $R = (2 + m_F/m_K)/5 = 0.78$ and where T_K and m_K are, respectively, the laboratory kinetic energy in the nucleus and rest mass of the K particle, and where T_F is the energy of a nucleon corresponding to the maximum momentum of a nucleon bound in a nucleus (~ 25 Mev) and m_F is its rest mass. The values of $\bar{\sigma}_{ub}$ for the three energy intervals of this experiment are listed in column 5 of Table V.

From $\bar{\sigma}_{ub}$, from the values for the charge-exchange/noncharge-exchange ratio f_c (corrected to refer to the primary K -nucleon collision and listed in Table V, column 6), and from the K -proton cross sections (taken from the results of recent counter experiments and listed in column 7 of the same table), the K -neutron cross sections for charge-exchange σ_{Kn^0} and noncharge-exchange σ_{Kn^+} have been evaluated. The following relationships were used:

$$\begin{aligned} \sigma_{Kn^0} &= [f_c/(f_c+1)] [\bar{A}/(\bar{A}-\bar{Z})] \bar{\sigma}_{ub}, \\ \sigma_{Kn^+} &= [\bar{A}\bar{\sigma}_{ub} - \bar{Z}\sigma_{Kp} - (\bar{A}-\bar{Z})\sigma_{Kn^0}]/(\bar{A}-\bar{Z}), \end{aligned}$$

where \bar{A} = average atomic weight, \bar{Z} = average atomic number. We used $\bar{A} = 100$ and $\bar{Z} = 44$. The values of σ_{Kn^0} and σ_{Kn^+} calculated separately for the three energy

²⁹ R. M. Sternheimer, Phys. Rev. **106**, 1027 (1957).

³⁰ The correction for the Pauli principle is only approximate. It is, however, small ($\lesssim 10\%$) and the effect of any inaccuracies of this correction is very small indeed.

intervals are listed in Table V, columns 8 and 9. The errors in these cross sections reflect the statistical uncertainty in the K -nucleon cross section as well as in the ratio f_c , and are the extended errors, i.e., the linear combination of both.

To obtain the corrected values f_c which were used, the experimentally observed charge-exchange/noncharge-exchange ratios, listed in Table III, were corrected for the following effects: (a) misclassification of inelastic noncharge-exchange events as elastic, (b) multiple collisions in the nucleus, and (c) the change of the Pauli-principle correction resulting from changes (see Sec. IIIC) in the K -neutron center-of-mass angular distribution. These corrections were made using a Monte-Carlo calculation discussed in Sec. IIID.

As was mentioned in Sec. IIIA, there is some uncertainty as to the values of r_0 and d which determine the Wood-Saxon potential. In that the nuclear density distribution is assumed to be of the same form, both W and ρ_0 should vary with changes in the values of r_0 and d . From the results of the UCLA group³ the variation of W is not strictly proportional to ρ_0 and therefore $\bar{\sigma}_W$ will change when other values of r_0 and d are assumed. The variation of the parameter r_0 from $1.07A^{1/3}f$ to $1.20A^{1/3}f$ would result in a 15% variation in the ratio W/ρ_0 . The resultant variation of the value of $\bar{\sigma}_W$ determined here would be +11% and -4%, respectively. These uncertainties have not been considered in the determination of the errors of $\bar{\sigma}_W$.

C. K -Neutron Differential Cross Sections from a Phase-Shift Analysis³¹

In this analysis we assume that K -nucleon scattering may be described in terms of orbital angular momentum states $l=0$ and $l=1$, i.e., scattering in terms of S and P waves. This assumption seems reasonable as a description of K -proton scattering, for the results indicate an approximate isotropic K -proton differential scattering cross section at 225-Mev K^+ energy,⁹ an angular dis-

³¹ This analysis follows along similar lines to an analysis of our data made recently by L. S. Rodberg and R. M. Thaler, Phys. Rev. Letters **4**, 372 (1960).

tribution consistent with isotropy at lower energies,² and a total scattering cross section that is approximately independent of energy in our energy range.^{9,32} Thus $K^+ - p$ scattering in this energy interval may be described as predominantly S wave with possibly a small P -wave contribution. The K -neutron charge-exchange scattering, as seen previously, is characterized by a total cross section increasing with K energy, indicating a contribution of higher angular momentum states; in this analysis we limit l to 1.

Ignoring in K -nucleon scattering the effect of the Coulomb field, assuming zero spin for the K meson and scattering in S and P waves only, the following amplitudes may be derived:

$$g_\alpha = a_S + (2a_{p3} + a_{p1}) \cos\theta^*,$$

$$g_\beta = (a_{p1} - a_{p3}) \sin\theta^* e^{i\phi},$$

where g_α is the coherent scattering amplitude, g_β is the incoherent spin-flip scattering amplitude, θ^* is the center-of-mass scattering angle of the K meson, ϕ is an arbitrary angle, and where the S - and P -wave scattering amplitudes are $a_S, a_{p,2j}$ ($j=l+s$), respectively. The complete description of the K -nucleon scattering processes must include the isotopic spin states $T=0$ and $T=1$ and their corresponding amplitudes a_0 and a_1 . Applying charge independence, the three scattering reactions may be characterized by the following amplitudes:

Scattering process	Isospin amplitude	
$K^+ + p \rightarrow K^+ + p$	a_1 ,	(4)
$K^+ + n \rightarrow K^+ + n$	$\frac{1}{2}(a_1 + a_0)$,	(5)
$K^+ + n \rightarrow K^0 + p$	$\frac{1}{2}(a_1 - a_0)$.	(6)

Expressing each angular-momentum amplitude in terms of the appropriate isospin amplitudes, the complete expressions for g_α and g_β for each reaction are obtained. The center-of-mass differential cross section for each process is then given by

$$d\sigma/d\Omega = (1/k_{c.m.}^2) (|g_\alpha|^2 + |g_\beta|^2)$$

$$= (1/k_{c.m.}^2) (A + B \cos\theta^* + C \cos^2\theta^*),$$

where $k_{c.m.}$ is the K -meson wave number in the center of mass of the K -nucleon system and where A, B , and C are expressions in the amplitudes. The total cross section is given by the integral of the above expression.

As a means of indexing for isotopic spin and angular momentum states, the method adopted is that used in pion physics, namely, the first index refers to the K -nucleon isotopic-spin state and the second to the angular momentum state. For S -wave scattering no second index appears. For P -wave scattering the second index

is twice the total angular momentum quantum number $j=l+s$.

The scattering amplitudes may be expressed in terms of the phase shifts, δ_{ij} , for which the same methods of indexing apply. The general relation may be written:

$$a_{ij} = e^{i\delta_{ij}} \sin\delta_{ij}.$$

In terms of these phase shifts the K -proton (or K -hydrogen) total cross section may be expressed as

$$\sigma_{Kp} = (4\pi/k_{c.m.}^2) (\sin^2\delta_{11} + \sin^2\delta_{11} + 2 \sin^2\delta_{13}). \quad (7)$$

The charge-exchange cross section may be written as follows:

$$\sigma_{Kn^0} = (\pi/k_{c.m.}^2) [\sin^2(\delta_1 - \delta_0) + \sin^2(\delta_{11} - \delta_{01}) + 2 \sin^2(\delta_{13} - \delta_{03})], \quad (8)$$

and the average K -nucleon total cross section may be written

$$\bar{\sigma}_{ub} = \left(\frac{4\pi}{k_{c.m.}^2} \right) \left[\frac{\bar{A} + \bar{Z}}{2\bar{A}} (\sin^2\delta_{11} + \sin^2\delta_{11} + 2 \sin^2\delta_{13}) + \frac{\bar{A} - \bar{Z}}{2\bar{A}} (\sin^2\delta_{00} + \sin^2\delta_{01} + 2 \sin^2\delta_{03}) \right], \quad (9)$$

where \bar{A} and \bar{Z} are the average atomic weight and number for emulsion nuclei.

In Sec. IIIA, the optical-model real and imaginary potentials V and W were determined. These may be related to the individual forward scattering amplitudes for K -nucleon scattering. The expression as derived by Riesenfeld and Watson,³³ Bethe,³⁴ and Kerman *et al.*³⁵ may be written

$$V + iW = -2\pi\rho_0 \bar{f}(0) (k_{lab}/k_{c.m.}) (\hbar^2 c^2 / E_K), \quad (10)$$

where, for a Wood-Saxon potential,²⁸

$$\rho_0^{-1} = 4\pi r_0^3 (1 + \pi^2 d^2 / r_0^2) / 3\bar{A},$$

and where the average K -nucleon forward scattering amplitude $\bar{f}(0)$, the laboratory wave number in K -nucleon scattering k_{lab} , and the total energy of K meson in the laboratory system E_K , refer to scattering inside the nucleus.

The average forward scattering amplitude may be written as follows:

$$\bar{f}(0) = \left(\frac{1}{k_{c.m.}} \right) \cdot \left[\frac{\bar{A} + \bar{Z}}{2\bar{A}} (a_1 + a_{11} + 2a_{13}) + \frac{\bar{A} - \bar{Z}}{2\bar{A}} (a_0 + a_{01} + 2a_{03}) \right].$$

Using, in Eqs. (7), (8), (9), and the real part of (10)

³³ W. Riesenfeld and K. Watson, Phys. Rev. **102**, 1157 (1956).

³⁴ H. A. Bethe, Ann. Phys. **3**, 190 (1958).

³⁵ A. K. Kerman, H. McManus, and R. M. Thaler, Ann. Phys. **8**, 551 (1959).

³² H. C. Burrowes, D. O. Caldwell, D. H. Frisch, D. A. Hill, D. M. Ritson, and R. A. Schluter, Phys. Rev. Letters **2**, 117 (1959).

TABLE VI. Best-fit solutions for phase shifts.

\bar{T}_K (Mev)	Average energy in nu- cleus (Mev)	Solu- tion	Phase shifts (radians)				Coefficients for differential cross sections					
			δ_1	δ_0	δ_{01}	δ_{03}	K-neutron charge-exchange			K-neutron noncharge-exchange		
							A	B	C	A	B	C
189	165	1	-0.48	-0.26	-0.25	0.28	0.08	0.008	-0.03	0.19	-0.07	-0.03
		2	-0.48	-0.24	0.45	-0.08	0.08	0.005	-0.04	0.18	-0.05	-0.04
257	233	1	-0.61	-0.12	-0.70	0.24	0.22	-0.09	-0.09	0.28	0.10	-0.09
		2	-0.61	-0.12	0.70	-0.24	0.22	-0.11	-0.09	0.28	0.12	-0.09
334	315	1	-0.74	0.52	-0.60	0.04	0.30	-0.21	-0.03	0.23	0.13	-0.03
		2	-0.74	0.20	0.60	-0.32	0.32	-0.20	-0.09	0.24	0.19	-0.09

the experimental K -nucleon cross sections and the previously derived real nuclear potential, the values for the phase shifts which satisfy these equations may be searched for. This set of four equations, however, is not sufficient to give a unique set of solutions for the six phase shifts.

In a recent counter experiment,⁹ K^+ -hydrogen scattering has been investigated at 225-Mev K energy. The preferred solution given for the S - and P -wave phase shifts is $\delta_1 = -0.58 \pm 0.04$, $\delta_{11} = -0.01 \pm 0.10$, and $\delta_{13} = 0.00 \pm 0.06$ radian. From these results it may be assumed that $\delta_{13} = \delta_{11} = 0$ and that $\delta_1 < 0$. Adopting this hypothesis, a search for values of δ_1 , δ_0 , δ_{01} , and δ_{03} which give cross sections and potentials within the experimental errors has been made. This was done with an IBM 704 computer, which searched for unknown phase shifts in a range from -1.0 to 1.0 radian in increments of 0.02 to 0.05 radian. The values which give a best fit to the experimental data are listed in Table VI. Two best-fit solutions were found at each energy. Also listed in this table are the corresponding values of the coefficients A , B , and C of the differential cross sections for the K -neutron reactions (2) and (3). (The K - p cross section is isotropic under the above assumptions.)

Qualitatively these results indicate a K -neutron charge-exchange differential cross section that is peaked forward (or nearly isotropic) at 190 Mev and is backwardly peaked at 260 Mev and at higher energies. The inverse follows for the K -neutron noncharge-exchange differential cross section. Considering all possible phase-shift solutions which result in values of σ_{Kn^0} , $\bar{\sigma}_{ub}$, and V lying within one standard deviation in error of each value, these qualitative conclusions are still valid; however, additional solutions giving near-symmetric angular distributions for both reactions at all energies are also possible but the values of χ^2 for these additional solutions are relatively large. A more quantitative conclusion does not seem possible. These results also confirm the existence of a P -wave contribution to scattering in the $T=0$ state. This follows from the fact that, within the rather large range of possible values of δ_{01} and δ_{03} , these phase shifts are never simultaneously zero.

The results of the above analysis were obtained

under the assumption of S -wave scattering in the $T=1$ state, as suggested by the results of Kycia *et al.*⁹ at 225 Mev. The K energy interval of this experiment, however, extends above this energy and thus a P -wave contribution is possible. Considering this possibility at $\bar{T}_K = 257$ Mev and 334 Mev, a further phase-shift analysis was made in which various values of δ_{13} within the interval -0.1 to 0.1 were assumed (δ_{11} was set to zero). The previous qualitative results were still found to be valid for δ_{13} in the interval -0.05 to $+0.1$.

It should be noted that Kycia *et al.* also give two alternative (but less probable) solutions for K - p scattering at 225 Mev, i.e., (a) $\delta_1 = -0.01 \pm 0.06$, $\delta_{11} = -0.60 \pm 0.04$, $\delta_{13} = -0.04 \pm 0.04$ and (b) $\delta_1 = 0.08 \pm 0.05$, $\delta_{11} = 0.62 \pm 0.05$, $\delta_{13} = 0.06 \pm 0.03$ radian. Were one of these solutions to be experimentally confirmed, a reanalysis of our data would be required, but this in turn would require further information on the energy dependence of the P -wave phase shifts for K^+ - p scattering.

Finally, these results, as well as those of Kerth *et al.*, were based on an analysis assuming scattering in S and P waves only. The validity of this assumption at these K energies has yet to be demonstrated.

D. Monte-Carlo Cascade Calculation

In this section, information has been sought on the K -nucleon cross sections, by an extension of the model of interaction described in Sec. IIIB, to include multiple collisions of the K meson in the nucleus, the nucleon cascade, and refraction at the nuclear boundary. In the calculation, proper account was taken of the varying K energy at which interactions occurred and the effect of the motion of the target nucleons in changing the center-of-mass energy and thereby the cross section. In this method, called the Monte-Carlo cascade calculation and first applied by Goldberger,³⁶ the K meson and recoil nucleons are followed as they traverse nuclear matter in a three-dimensional nucleus. Thus, event by event, the general characteristics of the interaction are summed up. This calculation was made using the Maniac II computer at the Los Alamos Scientific

³⁶ M. L. Goldberger, Phys. Rev. **74**, 1269 (1948).

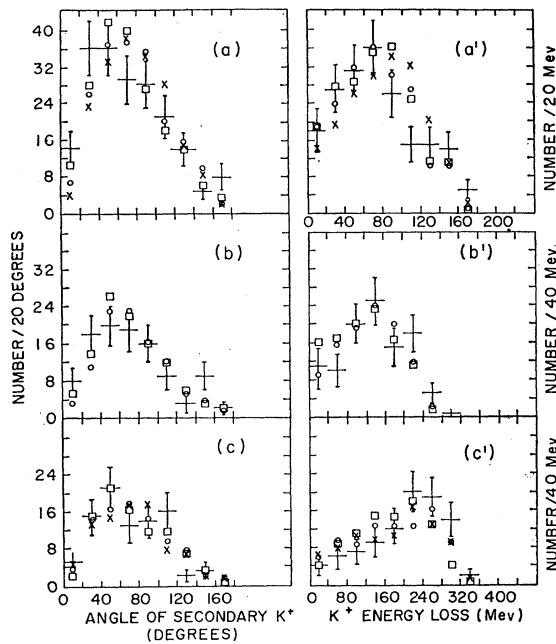


FIG. 8. Angular and energy-loss distributions of K^+ mesons from inelastic K -nucleus scattering. (a) and (a') correspond to average K energy 189 Mev, (b) and (b') to 257 Mev, and (c) and (c') to 334 Mev. Experimental results, with corresponding errors, are compared with Monte-Carlo calculations which have as symbols \circ , \times , and \square corresponding, respectively, to trials 1, 2, and 3 (see Table VII).

Laboratory. The computer program was that of Sartori, Werbrouck, Wooten, and Bivins; it has recently been described in a Princeton University report.³⁷

In this calculation the momentum distribution for nucleons used was that suggested by Frances, Eden, and Brueckner³⁸:

$$P(p_F)dp_F \propto p_F^2 \exp(-p_F^2/p_0^2)dp_F,$$

where $p_0^2 = 2m_F T_0$; $T_0 = 14$ Mev. As input information, the previously computed K -nucleon total cross sections and real nuclear and Coulomb potentials were used. For the three trial calculations, three sets of K -nucleon center-of-mass differential cross sections were assumed for K particles in the energy range of this experiment. The distributions are listed in Table VII.³⁹ For K particles at energies less than 100 Mev, all three reactions were assumed to be isotropic.

For other K reactions that occur in nuclear matter, charge symmetry was used to equate their cross sec-

³⁷ L. Sartori, A. E. Werbrouck, J. Wooten, and R. Bivins, The Monte Carlo Calculation, Elementary Particles Laboratory Internal Report, Princeton University, November, 1959 (unpublished).

³⁸ N. C. Frances, R. S. Eden, and K. A. Brueckner, Phys. Rev. **98**, 1445 (1955). The distribution as it was applied resulted in bound states with positive energies. A more satisfying but less realistic distribution would be $P(p_F) \propto p_F^2 dp_F$.

³⁹ The alternate choice of forward and backward distributions in trials 2 and 3 as well as the inclusion of the SB distribution was dictated by considerations of the previous section on phase-shift analysis.

TABLE VII. Assumed angular distributions for Monte-Carlo calculation.^{a, b}

Trial	Reaction		
	(1), Kp^+	(2), Kn^+	(3), Kn^0
1	I	I	I
2	I	B	F
3	SB	F'	B'

^a See reference 39.

^b I indicates an isotropic angular distribution, F a forward angular distribution of the form $0.048 + 0.138 \cos\theta + 0.136 \cos^2\theta$, B a backward angular distribution of the form $0.112 - 0.214 \cos\theta + 0.126 \cos^2\theta$, F' a forward angular distribution of the form $1 + \cos\theta$, B' a backward angular distribution of the form $1 - \cos\theta$, and SB a slightly backward distribution of the form $1 - 0.2 \cos\theta$.

tions to the experimentally determined differential and total cross sections. For the nucleon-nucleon total and differential cross sections, the most recent experimental results were used.⁴⁰

Comparisons between the Monte-Carlo calculations and the corresponding experimental distributions are shown in Figs. 8 and 9. These figures show the K -energy loss, the angular distributions for secondary K^+ mesons, and the energy distributions for protons having energy greater than 40 Mev.⁴¹ In general, the number of Monte-Carlo events is three to four times the number of events experimentally observed. The statistical errors, in percent, for the calculated points are, therefore, approximately one-half those shown for the experimental points.

In each figure the curves (and tables) were normalized to correspond to the total number of experimentally observed events. This was found necessary because, in these calculations, the total K -nucleon cross sections were not adjusted to correct for the effect of the Pauli principle which, when the center-of-mass angular distribution was changed, altered the effective total cross section.

Due to the assumed nucleon momentum distribution and the way in which it was applied, positive-energy states for nucleons in the nucleus were allowed. This resulted in events in which the K particle gained energy in a nuclear encounter. These events, which were about 4% of all inelastic interactions, were eliminated from the results of the calculations.⁴² Also, in some cases, events, appeared in which the sum of the energies of

⁴⁰ W. N. Hess, Revs. Modern Phys. **30**, 368-401 (1958).

⁴¹ For proton energies less than ~ 30 Mev, the process of nuclear evaporation becomes more and more important. This process was not considered in the Monte-Carlo calculation. It was also not considered in this analysis, as it is only distantly related to the K -nucleon interaction.

⁴² This procedure was adopted after comparing the results of two Monte-Carlo calculations for incident protons at 140 Mev, one using a Gaussian momentum distribution [$p_F^2 \exp(-p_F^2/p_0^2) dp_F$] and the other a Fermi nucleon momentum distribution ($p_F^2 dp_F$). The Fermi distribution results in no positive energy states for nucleons and therefore energy conservation in K nucleus interactions is assured. The procedure of eliminating protons which gained energy in primary encounters from the results obtained using the Gaussian distribution, was effective in reducing the number of events at forward angles to the point where the results of both calculations were approximately the same.

secondary particles was greater than the incident energy. These events were not eliminated. Their inclusion no doubt resulted in an increased average energy for secondary particles from these interactions.

In comparing the results from the three trials which are shown in Figs. 8 and 9, one notes their striking similarity to each other and in turn their close similarity to the experimental results which are also shown. This affirms the validity of the method but also its insensitivity. The insensitivity can be explained, in part, by the effect of the nucleon momentum in changing the direction of the motion of the center of mass and by multiple collisions of K mesons in emulsion nuclei which occurs in 30 to 40% of the K -nucleon interactions. It is nevertheless surprising that even gross changes in the K -neutron angular distributions have such a small effect.

Given the insensitivity of this method, no further attempts were made to improve on the calculation by the elimination of the difficulties previously mentioned. The calculation, however, has furnished a means of estimating the number of undetected inelastic events. This was accomplished by the selection of those Monte-Carlo events (without cascade proton emission) which could have been lost because the scattering angle of the K^+ meson was small and the K^+ energy loss was too low to be experimentally detected. An equivalent number of events, after normalization, were added both to the energy-loss distribution and to the angular distributions experimentally observed. The corrected points are shown in Figs. 8 and 9. The equivalent numbers of experimental events for the three energy intervals are given in Sec. IIIA where they were used to correct the total inelastic K -nucleus cross sections and consequently the values of W . They represent the maximum number of events that was consistent with the results of the Monte-Carlo calculation. These events, when added to the experimental data, not only change the total inelastic cross sections, but also the charge-exchange/noncharge-exchange ratios. These modified experimental ratios f are compared with the corresponding ratios obtained from the Monte-Carlo calculation in the tables of Fig. 9. Also in these tables the corrected values of the number of protons per star \bar{N}_p , and of the average proton energy per star \bar{T}_p , are compared with the corresponding calculated values.

The Monte-Carlo calculation also furnished a means of correcting for the effect of multiple collisions and of the Pauli principle in altering the charge-exchange/noncharge-exchange ratio. Considering those Monte-Carlo results which refer to the same form of angular distribution as predicted by the phase-shift analysis, a correction was deduced by comparing the charge-exchange/noncharge-exchange ratio at the first collision in the nucleus, f_c , with the ratio f resulting from multiple collisions. The correction factor by which f must be multiplied was found to be 0.83 for the lowest energy ($\bar{T}_k=189$ Mev), 0.80 for the intermediate

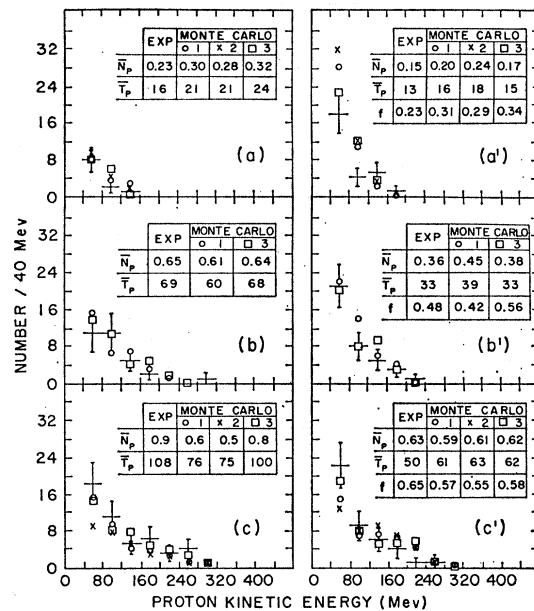


FIG. 9. Energy distributions of secondary protons of kinetic energy ≥ 40 Mev from inelastic K^+ -nucleus scatterings; (a), (b), and (c) refer to protons from charge-exchange events and (a'), (b'), and (c') to protons from noncharge-exchange events. The corrected experimental results are presented along with those obtained from a Monte-Carlo calculation in which the symbols \circ , \times , and \square correspond, respectively, to trials 1, 2, and 3 (see Table VII); (a) and (a') refer to average K energy 189 Mev, (b) and (b') to 257 Mev, and (c) and (c') to 334 Mev. In the tables, the average number of protons per event, \bar{N}_p , the average energy of these protons per event, \bar{T}_p , and the ratio of charge-exchange/noncharge-exchange scattering, f , are also given along with the corresponding experimental values which were corrected for misclassification of events.

energy ($\bar{T}_k=257$ Mev), and 0.76 for the highest energy ($\bar{T}_k=334$ Mev). These corrected ratios f_c are listed in column 7 of Table V and refer to the primary K -nucleon collision in the nucleus.

E. Pion Production by K^+ Mesons

The threshold for pion production in K^+ -nucleon encounters is 225 Mev if the target nucleon is at rest. In nuclei, interactions of K^+ mesons occur with nucleons which are in motion, and therefore π mesons may be produced at lower K -meson laboratory energies (albeit with a sharply diminishing cross section). Thus, in K -nucleus interactions the π mesons may be produced at K energies as low as ~ 200 Mev.

In the careful examination of all K inelastic scatterings and K decays, one event has been found in which a pion was produced. The details of the event have been discussed in Sec. IIF where the values of primary and secondary energies are given.

Two other events have also been reported, one by the Padova group,⁴³ and one by the UCLA group.⁴⁴ They

⁴³ M. Grilli, L. Guerriero, M. Merlin, Z. O'Friel, and G. A. Salandin, *Nuovo cimento* **10**, 163 (1958).

⁴⁴ E. Helmy, J. H. Mulvey, D. J. Prowse, and D. H. Stork, *Phys. Rev.* **112**, 1793 (1958).

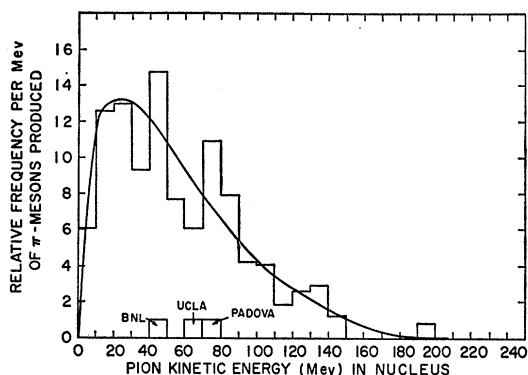


FIG. 10. Energy spectrum in the nucleus for π mesons produced in K^+ -nucleon encounters. The histogram and curve were deduced from a Monte-Carlo phase-space calculation. The three observed events are also shown.

were also interpreted as having resulted from a K -neutron interaction.

From a Monte-Carlo phase-space calculation, the average momentum distribution of π mesons created in the nucleus has been determined. The energy spectrum, which is shown in Fig. 10, was obtained as the sum of spectra produced at all observed K energies weighted by the number of inelastic events per K energy interval observed at Padova, Dublin, UCLA, and BNL. The π energies for the observed events, which are also shown in the figure, were corrected to refer to energies inside an average emulsion nucleus.⁴⁵ These π energies are not far from the maximum of the calculated distribution.

In estimating the cross section for π production, the efficiency of observation must be considered as well as the effect of absorption and trapping of π mesons in the potential well of the nucleus in which they are produced. Roughly, the detection efficiency for π -meson observation may be estimated to be $\sim 70\%$ and the probability of escape from the nucleus was estimated to be $\sim 70\%$.^{46,47} From these values the K -nucleon cross section for charged π production at an average K energy of ~ 280 Mev has been estimated to be $\sim 1/7$ mb.

IV. CONCLUSIONS

1. The real K^+ -nuclear potential V was found to be repulsive (positive). Assuming a Wood-Saxon potential with parameters $r_0 = 1.15A^{1/3}$ f and $d = 0.57$ f, the value of V was found to vary from 18.5 ± 3.3 Mev in the lowest energy interval to 13.5 ± 5.0 Mev at the highest energy, but, given the experimental errors, could be considered as virtually constant over this energy range.

⁴⁵ Values for the pion nuclear potential for varying pion energies were kindly furnished by R. M. Sternheimer. [See R. M. Sternheimer, Phys. Rev. **101**, 384 (1956).]

⁴⁶ A. Minguzzi and A. Minguzzi-Ranzi, Nuovo cimento **10**, 1100 (1958).

⁴⁷ J. H. Hornbostel and G. T. Zorn, Phys. Rev. **109**, 165 (1958).

In the same interval the imaginary nuclear potential W changed from -12.9 ± 1.4 Mev to -17.6 ± 2.5 Mev.

2. The average K -nucleon total cross section was found to increase slowly with increasing K energy. The charge-exchange cross section is strongly energy dependent, having a value of 4.6 ± 1.2 mb at 165 Mev and of 10.3 ± 2.4 mb at 315 Mev. This indicates P -wave scattering in the $T=0$ state at highest energy and this conclusion is confirmed in the phase-shift analysis.

3. From the phase-shift analysis, the increase in the charge-exchange cross section seems to be accompanied by a change in the K -neutron center-of-mass angular distribution for charge exchange. The distribution changes from predominantly forward or near symmetric to predominantly backward in the energy interval between 165 Mev and 233 Mev. The K -neutron noncharge-exchange differential cross section varies from backward or near symmetric to predominantly forward. These results, however, are tentative (see Sec. C).

4. The results of the phase-shift analysis are not in contradiction with those of the Monte-Carlo calculation, which is generally found to be insensitive even to gross changes in the differential K -neutron scattering distributions.

5. One example of pion production has been observed, and the K -nucleon cross section for this process at an average K energy of 280 Mev has been estimated to be $\sim 1/7$ mb.

6. No evidence has been found for violation of the theoretical schemes which were taken as a basis for the K^+ -nucleon interaction.

ACKNOWLEDGMENTS

For the exposure of the emulsion stacks we would like to express our appreciation to the staffs of the Brookhaven Cosmotron and of the Berkeley Bevatron, and in particular to Dr. G. Collins and Dr. E. Lofgren for their cooperation. We would also like to thank Dr. D. Meyer for his participation in the design and setting up of the separated K^+ beam at the lowest K momentum, and Dr. D. H. Stork and Dr. J. H. Mulvery for their generous help in making the exposure of the two emulsion stacks at higher momentum in the separated K^+ beam designed by them.

We are indeed grateful for the assistance of Mrs. M. Hall, J. Greener, Mrs. V. Austen, Mrs. B. Cozine, Mrs. O. Oldenbusch, Mrs. J. Reidl, and Mrs. A. Biittner, who enthusiastically and diligently scanned for and then analyzed the K^+ events reported in this investigation. We would also like to acknowledge the aid of J. Smith in making multiple-scattering measurements and of J. Quinn in preparing the exposures.

In the interpretation of the experimental results, we are indebted to Dr. G. Igo for furnishing the computer program for the optical-model calculation and for his aid in adapting it to the IBM 704 computer used by Brookhaven.

The Monte-Carlo cascade calculation was made possible by the cooperation of the Los Alamos Scientific Laboratory, and by the generous help and cooperation of Dr. L. Sartori and Dr. A. Werbrouch, J. Wooten, and R. Bivens in applying their program to the analysis of our experimental data.

Finally we would like to express our sincere thanks to Dr. E. O. Salant, Dr. J. Cronin, and in particular Dr. J. Hornbostel and Dr. R. M. Sternheimer for criticisms and many helpful discussions.

APPENDIX

The computer calculation that was made was an exact calculation using a partial wave expansion of the Schrödinger wave equation. The method is discussed in a number of texts.⁴⁸

In determining the relativistic corrections, the Schrödinger radial wave equations for a central Coulomb field,

$$\frac{1}{r^2} \frac{d}{dr} \left(r^2 \frac{dR}{dr} \right) + \left[\frac{2m_K T_K}{\hbar^2} - \frac{2m_K Z e^2}{\hbar^2 r} - \frac{l(l+1)}{r^2} \right] R = 0,$$

was compared with the corresponding relativistic

equation,

$$\frac{1}{r^2} \frac{d}{dr} \left(r^2 \frac{dR}{dr} \right) + \left[\frac{p_K^2}{\hbar^2} - \frac{2E_K Z e^2}{\hbar^2 c^2 r} - \frac{l(l+1)}{r^2} \right] R = 0,$$

derived from the Klein-Gordon equation.⁴⁹ In the latter derivation the nuclear potential was assumed to be small in relation to the incident K energy E_K . The suggested corrections to the nonrelativistic equation are to replace $m_K c^2$ (the K -meson rest mass) with E_K (the total K energy, $T_K + m_K c^2$) and T_K by $T_K \cdot [(T_K + 2m_K c^2)/2E_K]$.

In a prior calculation the WKB approximation was applied in determining the phase shifts for the Klein-Gordon equation, using the method of Gatha and Riddell.⁴⁹ This method was modified to include a Wood-Saxon potential as suggested by Sternheimer.⁵⁰ The results of this calculation compare quite closely with the elastic differential cross section as determined from the exact solution of the Schrödinger equation with relativistic corrections. The maximum deviation of the results of the WKB method occurred in the interference regions and gave a value for the cross section $\sim 15\%$ higher than that obtained with the exact solution.

⁴⁸ See, for example, L. I. Schiff, *Quantum Mechanics* (McGraw-Hill Book Company, Inc., New York, 1949), pp. 119-120.

⁴⁹ K. M. Gatha and R. J. Riddell, Jr., *Phys. Rev.* **86**, 1035 (1952).

⁵⁰ R. M. Sternheimer, *Phys. Rev.* **97**, 1314 (1955).